doi: 10.15407/ujpe61.09.0812

V.S. SAVENKO, G.M. VERBINSKA, L.A. BULAVIN

Taras Shevchenko National University of Kyiv
(64, Volodymyrs'ka Str., Kyiv 01601, Ukraine; e-mail: volodymyr.savenko@ukr.net)

COMPUTER SIMULATION OF EVAPORATION PROCESS OF NaCl AQUEOUS SOLUTION

PACS 71.20.Nr, 72.20.Pa

The evaporation of aerosol droplets is an important aspect of industry and science. Although the theoretical background of this process was developed more than one century ago and is complemented nowadays by various corrections, its formulas are not completely relevant for the evaporation process: they often give just crude estimations for complex systems. The computer simulation is an appropriate tool for the calculation of parameters of the evaporation of aerosols. In this paper, we present a model for the computer simulation of the evaporation of ionic solutions. Salt NaCl is chosen for the role of electrolyte due to its simplicity and widespread application. The simulation process is based on the Monte-Carlo method. We consider the temperature T, pressure of the environment P, and NaCl concentration as income parameters of the simulation and the evaporation coefficient as an outcome one. To simulate the interaction between water molecules, the Stockmayer and Lennard-Jones potentials are used. To estimate the efficiency of the proposed model, the evaporation coefficient was measured experimentally. It is shown that the experimentally obtained evaporation coefficients have the same order of magnitude as ones calculated by means of the computer simulation.

K e y w o r d s: computer simulation, evaporation process, NaCl aqueous solution, Monte-Carlo method.

1. Introduction

The aim of this work is the development of an appropriate model for the simulation of the evaporation of a water-based electrolyte solution. In this investigation, we used a NaCl aqueous solution. This choice is due to the facts that the H_2O–NaCl system is one of the most common solutions, and sodium and chlorine ions are monovalent and have a spherical symmetry. Nevertheless, the model could be adapted to describe more complicated systems. The relevance of this work is due to the wide use of the aqueous solution in various fields of industry, medicine, pharmacology, *etc.* Such studies are essential for a further improvement of the theory of evaporation and condensation in order to clarify the physical mechanisms that enforce them and for the development of appropriate theoretical models. Moreover, the results of this work could lead to a new approach to the estimation of the evaporation parameters for complex systems, which would allow one to control the evaporation and the condensation more precisely.

The specific phase transformation, including the evaporation, occurs at a certain rate that depends on conditions, under which the phase transition takes place. The simplest case is the evaporation from a liquid surface into vacuum. If a liquid is in a closed vessel, the saturated vapor is formed over its surface, and a dynamic equilibrium is established, at which the number of molecules leaving the liquid surface is equal to that of molecules going from the vapor back to the liquid surface. The number of molecules that

condense on a unit area of the liquid surface per unit time is expressed by the well-known formula for the kinetic evaporation regime:

$$\frac{dN}{dt} = \alpha\Omega n\frac{v}{4}, \tag{1}$$

where n is the concentration of vapor molecules, α is the evaporation coefficient, Ω is the droplet surface area, and v is the average thermal velocity of vapor molecules. In many real cases, the evaporation of liquid occurs in the presence of another (background) gas. Then the molecules that left the liquid cannot go far away from its surface due to their collisions with molecules of the background gas. Molecules of the evaporating substance diffuse away from the liquid surface. This process is called the diffusion regime of evaporation. The rate of diffusion evaporation of a droplet with radius r is determined by the Maxwell formula [1]:

$$I_{\rm m} = -\frac{dm}{dt} = 4\pi D\,(C_0 - C_\infty), \tag{2}$$

where $I_{\rm m}$ is a change of the droplet mass per unit time, D the diffusion coefficient of the liquid vapor in the background gas, C_0 is the concentration of the saturated vapor at the droplet temperature, and C_∞ is the vapor concentration at the infinite distance from the droplet, which is determined by the humidity. Supposing the droplets to be spheres with density ρ and surface area S, the evaporation rate can be expressed by the formula

$$-\frac{dS}{dt} = \frac{8\pi D}{\rho}\,(C_0 - C_\infty), \tag{3}$$

There are a few corrections, which take real experimental conditions into account, and they need to be introduced into the Maxwell formula for a better precision. The most significant one is the Fuks correction, which considers the vapor concentration shift between the kinetic and diffusion evaporation regimes. The second important amendment is a correction related to the Stefan flow, which considers the presence of the environmental gas flow. It compensates pressure changes due to the water vapor flow from the droplet. Moreover, there are corrections which consider a non-spherical form of the suspended droplet and the presence of a convection. But their impacts are not as significant as two first corrections. Hence, with regards for the mentioned corrections, the evaporation rate is determined by the following formula [1]:

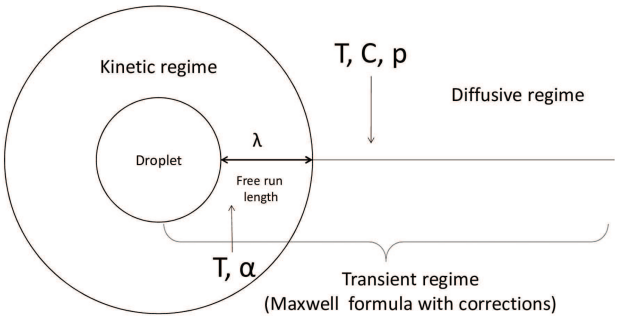

Fig. 1. Regimes of evaporation from the droplet surface

$$-\frac{dS}{dt} = \frac{8\pi D}{\rho}\,(C_0 - C_\infty)\left(\frac{D}{ru\alpha} + 1\right)^{-1} \times \times \left(1 + \frac{P_0 + P_\infty}{2P}\right), \tag{4}$$

where the first additional multiplier corresponds to the Fuks correction, D is the diffusion coefficient, r is the droplet radius, and u and α are the average velocity and the condensation coefficient of water vapor molecules, respectively. The second multiplier corresponds to the Stefan-flow correction, where P_0 and P_∞ are the partial pressures of water vapor at the droplet surface and at infinity, respectively, and P id the total pressure of the environment. Using this formula, we have approximated the experimental dependences of the droplet evaporation rate on the reciprocal pressure. This allowed us to determine the condensation coefficient α of the studied liquid.

2. Experimental Measurements

The scheme of experimental facilities for the evaporation rate measurement is presented at Fig. 2. Chamber (2) used to study the evaporation of suspended droplet (1) have form of a horizontally oriented cylinder. A thermostat liquid was circulating between the double walls of a cylinder. The thermostat keeps the temperature in the chamber to be constant in the range of 5–40 °C with ±0.1 °C deviation.

The temperature in the chamber was monitored by a temperature sensor. For this purpose, we used the p-n junction of a chip transistor. This allowed the inertia of the system for the temperature monitoring to be considerably reduced. The electronic system allowed us to measure the temperature with an accuracy of ±0.03 °C, and another similar sensor was used

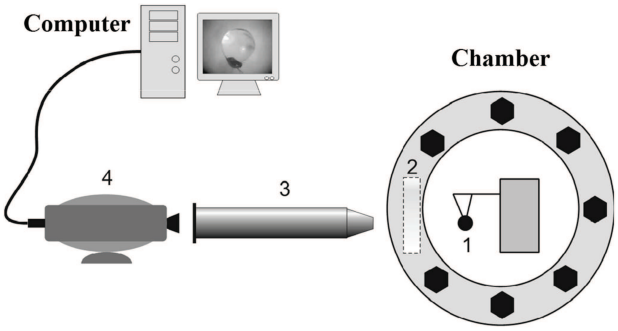

Fig. 2. Experimental equipment for the measurement of the of liquid droplets evaporation rate. *1* – droplet of the studied liquid, *2* – chamber, *3* – optic lens, *4* – digital camera

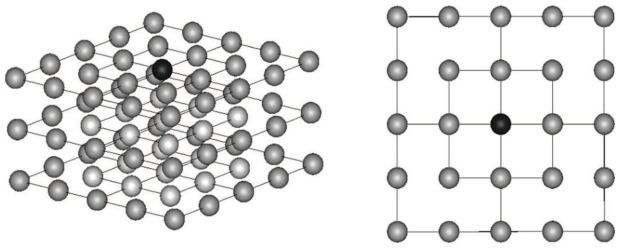

Fig. 3. Lattice model of water structure. Each node is occupied by a water molecule or salt ion

to monitor the droplet temperature. To make a contact with the liquid better, the sensor was also used as the bracket for a droplet. It should be noted that the simultaneous application of the *p-n* junction of a chip transistor as a bracket and a temperature sensor allowed us to substantially reduce the heat conductivity through the bracket and approach the conditions of free droplet evaporation much closer in comparison with the traditional technique of temperature measurements with the help of a thermocouple.

The chamber has hermetically built-in glass windows, which allow us to illuminate a liquid droplet and observe its evaporation process. The suspended droplet is regularly photographed after a certain time interval by a digital camera located outside the vacuum cylinder and supplied with a specially selected lens (3). For qualitative measurements, it is necessary to keep the appropriate illumination regime, which makes the dark droplet edge to be clearly distinguished on the white background. A wire with calibrated thickness was located near the droplet to provide the proper scaling of the photo. Since the temperature and the photos were registered with the help of the same computer, the computer clock was used for the time scaling. The further images of the liquid droplet during the evaporation process are processed by the MATLAB algorithm in order to register droplet surface changes with time.

3. Computer Simulation

For the simulation of the salt water solution evaporation, the lattice model (Fig. 3) was used in order to simplify the calculation of parameters of the model. The lattice model of water structure was previously used in [2,3]. In this model, the solution is represented as a set of water molecules and salt ions, which are located at equal distance from each other. This distance was calculated in accordance with the droplet temperature. Only several upper layers of the solution were taken into account (the reason for such approach will be discussed below).

The cells were randomly filled with salt ions and water molecules with regard for the concentration of NaCl. The orientations of water molecules were determined by the nearest salt ion. Then the potential barriers for surface water molecules and, as a result, the possibility of their leaving of the liquid surface were calculated. To avoid the edge effects, only the internal molecules were checked for this possibility. The ratio between the numbers of molecules, which left surface, and ones, which stayed on it, is considered as the evaporation coefficient.

We consider that the evaporation occurs in the kinetic regime at distances not exceeding the mean free path of water molecules in the gaseous state. In this case, we should not consider the impact of the environment on the process of saline evaporation. In this mode, we are able to derive the evaporation coefficient α, which affects both the kinetic regime and, more realistically, the transitional regime.

The evaporation coefficient was calculated in following way. For each water molecule located in the surface layer of the solution, we calculated the energy of interaction with neighboring molecules and ions. We assume that a water molecule turns into a gaseous state with a certain probability W in a way similar to the Ising model [4]. The probability of such transition is determined by the Landau–Lifshitz equation for fluctuations in a closed system [5]:

$$W = \exp\left(\frac{-U_b}{kT}\right), \tag{5}$$

where U_b is the potential barrier, and kT is the thermal energy.

The value of U_n was calculated after several iterations. On the first one, we count the interaction potential energy only with nearest water molecules. We considered their sum as U_1. On the second iteration, we include the interaction with the second layer of neighbor molecules. As a result, the second iteration potential consists of the interaction energy with molecules of the first and second layers, and so on. Hence, we obtain the sequence of potential energy barrier values: U_1, U_2, U_3, ... (Fig. 4).

This sequence converges to a limited value U_b, since the number of neighbors increases at each iteration step as n^2, whereas the intermolecular interaction potential energy decreases as $1/n^6$. This assumption is valid in the case of the 6–12 potential of intermolecular interaction between water molecules. So, for the simulation, we used only such type of potentials. To estimate the complete potential barrier U_b, we used the following formula:

$$U_b = U_n \left(1 - \exp\left(-a\, n\right)\right). \tag{6}$$

The complete potential energy barrier U_b comprises the interaction with neighbor water molecules and with salt ions Na^+ and Cl^-. The second term was estimated by the simple dipole – point charge interaction formula:

$$U_{d-i} = |\mathbf{p}||\mathbf{E}| \cos\theta, \tag{7}$$

where $\mathbf{p}$ is the dipole moment (its value for a water molecule was taken from [9]), $\mathbf{E}$ is the electric field intensity created by the point charge of a salt ion, and θ is an angle dipole and electric field intensity vectors. To increase the precision, the Debye screening effect was taken into account. The effective salt ion electric potential was assumed to be

$$U_{d-i} = -\mathbf{pE} \exp\left(\frac{-r}{r_{\mathrm{D}}}\right) = |\mathbf{p}||\mathbf{E}| \cos\theta \exp\left(\frac{-r}{r_{\mathrm{D}}}\right), \tag{8}$$

where r_{D} is the Debye screening length.

Different potentials of intermolecular interaction were used to calculate the potential energy barrier for surface water molecules. As the first approximation, we used the bare Lennard-Jones potential:

$$U\left(r\right) = 4\epsilon \left(\frac{\sigma^{12}}{r^{12}} - \frac{\sigma^6}{r^6}\right), \tag{9}$$

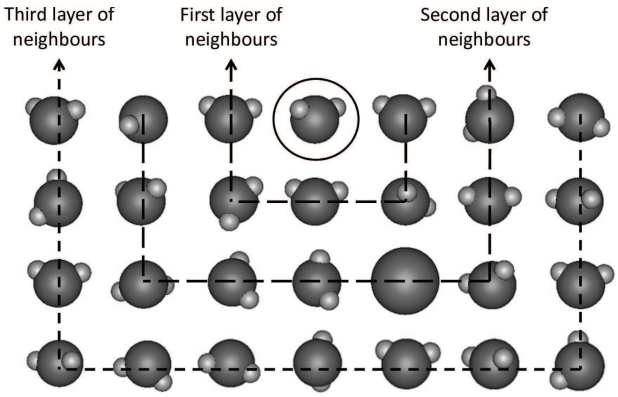

Fig. 4. Layers of neighbor molecules and ions

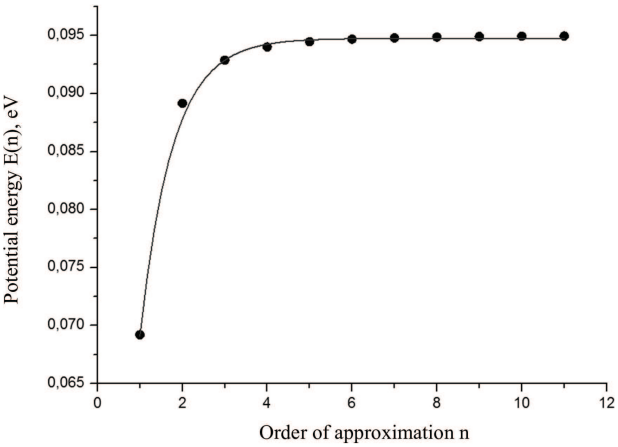

Fig. 5. Sequence of U_n converges to a certain value of potential barrier U_b

where ϵ and σ are energetic and distance parameters, which were taken from [6–8].

We also used the anisotropic Stockmayer potential, which is based on the above-mentioned 6–12 Lennard-Jones potential, but it involves the dipole-dipole interaction between water molecules:

$$U\left(r, \theta_a, \varphi_a, \theta_b, \varphi_b\right) = 4\epsilon \left(\frac{\sigma^{12}}{r^{12}} - \frac{\sigma^6}{r^6}\right) - \\ - \frac{d_a d_b}{r^3} g\left(\theta_a, \theta_b, \varphi_a - \varphi_b\right), \tag{10}$$

where θ and φ are the polar and azimuth angles of dipoles, respectively, g is the angle function:

$$g\left(\theta_a, \theta_b, \varphi_a - \varphi_b\right) = 2\cos\theta_a \cos\theta_b - \\ - \sin\theta_a \sin\theta_b \cos\left(\varphi_a - \varphi_b\right), \tag{11}$$

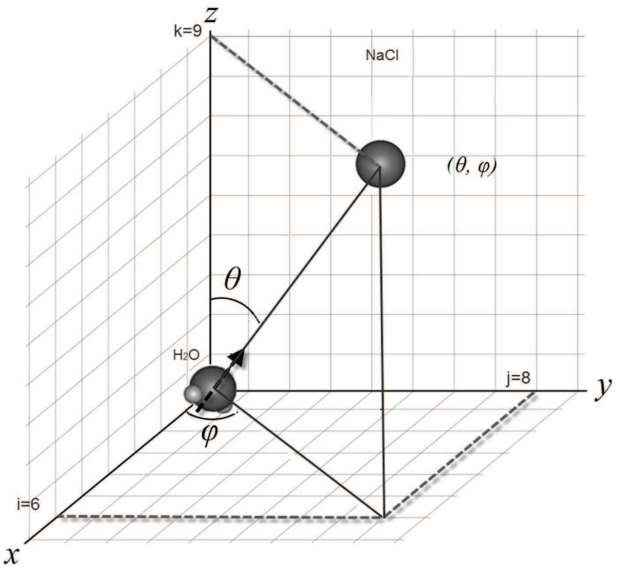

Fig. 6. Direction of the water molecule dipole determined by polar and azimuth angles

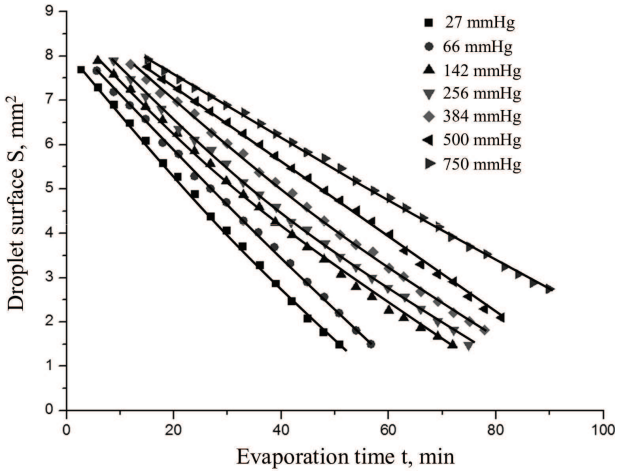

Fig. 7. Dependences of droplets' surfaces on the time for the initial concentration of NaCl, pressures in the interval 27–750 mmHg, and a temperature of 20 °C

In the case of the Stockmayer potential, the assumption of the spherical symmetry of water molecules could not be applied. Therefore, we introduce the direction of water molecules. The dipole vectors of water molecules are determined by the nearest salt ion electric field (Fig. 6). In our model, its direction could also be represented by the relative position of a salt ion cell.

4. Results and Discussion

To check the results of the computer simulation, the experimental measurements of the evaporation rate of NaCI water solution droplets at different initial concentrations and temperatures were carried out. Using the experimental equipment described above, we measured the evaporation rate in the intervals of concentrations C_s = (0.1–2.5)% and environment pressures of 27–760 mmHg. Our main aim was to derive the evaporation coefficient from these experimental results. The derivation of this parameter consisted of a few stages. At the first one, we measured the changes in the surface of droplets with the

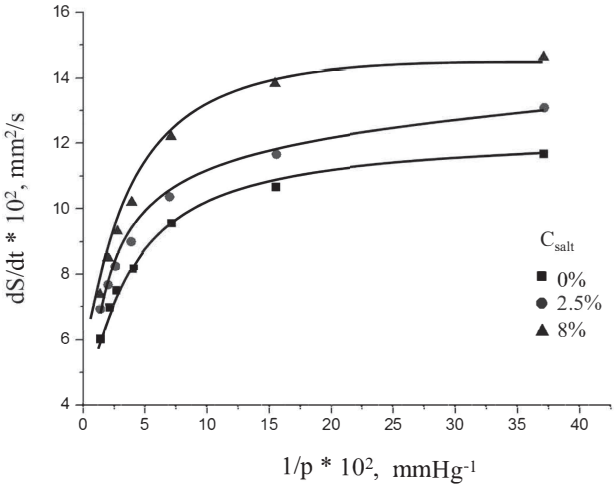

Fig. 8. Evaporation rate of a water NaCl solution versus the environment pressure at various concentrations of salt

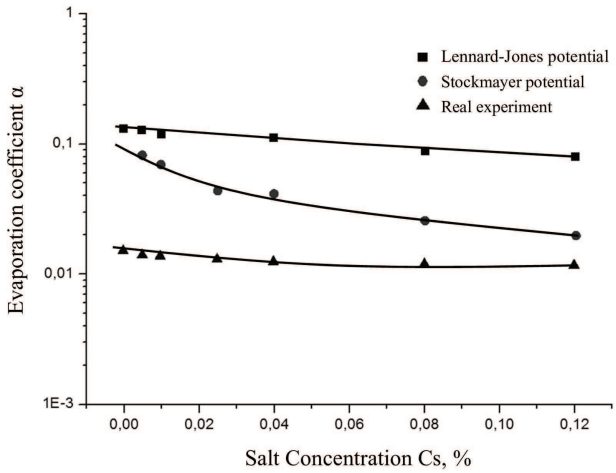

Fig. 9. Comparison of the evaporation coefficients, which were obtained experimentally and by computer simulations

time at the different initial salt concentrations and environment pressures (Fig. 7).

Then we calculated the instant evaporation rate $\frac{dS}{dt}$ at various time moments, by considering the fact that the salt concentration in a droplet increases during the evaporation, since some part of water molecules has left the liquid surface. Thus, we obtained the data set of pairs ($\frac{dS}{dt}$, C_s) for various environmental pressures. As a result, we were able to construct the dependences between the evaporation rate dS/dt and the inverse environmental pressure (used for a more convenient analysis of data) at various salt concentrations (Fig. 8).

At the final step of the derivation, we approximate the dependences of the NaCl water solution evaporation rate on the inverse environmental pressure by formula (4) at various salt concentrations. The evaporation coefficient α was considered as an adjustment parameter. As a result, we estimated the value of α, which corresponds to the certain values of the salt concentration (Fig. 9).

In the course of the evaporation process simulation, we initialized the lattice model configuration at each Monte-Carlo iteration, by using the salt concentration and the temperature as initial parameters. After the derivation of the potential barrier for each water molecule, we check its possibility to leave the liquid surface. Thus, we calculated the evaporation coefficient at various salt concentrations, which numerically equals to the averaged ratio between the number of water molecules, which have left the liquid surface, and the complete amount of molecules. As was mentioned above, two types of potentials were used: the Lennard-Jones and Stockmayer ones.

The comparison of the experimentally measured evaporation coefficients of the NaCl water solution and those obtained by means of the computer simulation were used to estimate the relevance of the proposed lattice model (Fig. 9).

5. Conclusions

Two types of intermolecular potentials are used for the simulation of the evaporation process, namely the Lennard-Jones and Stockmayer potentials. For each potential, the dependence of the evaporation coefficient on the salt concentration is derived. The results of the computer simulation and the experimental measurements are presented in Fig. 9.

The values of evaporation coefficient obtained by means of the computer simulation have the same order of magnitude as ones obtained experimentally. This fact indicates the relevance of the proposed model for the evaporation of a NaCl aqueous solution.

As is seen from Fig. 9, the better matching with experimental data was provided by the Stockmayer potential. This result can be explained by the fact that it takes into account the dipole moment of water molecules, in contrast to the Lennard-Jones potential.

In order to increase the accuracy of the proposed model, the H-bonds should be considered. In this case, the Lennard-Jones potential parameters need to be adjusted.

The authors thank A.M. Grygoriev for his help with the article.

1. N.A. Fuks, *Evaporation and growth of droplets in a gaseous medium* (USSR Acad. Sci. Publ. House, Moscow, 1954) (in Russian).
2. M. Pretti and C. Buzano, Thermodynamic anomalies in a lattice model of water, *J. Chem. Phys.* **121**, 11856 (2004) [DOI: 10.1063/1.1817924].
3. S. Succi, N. Moradi, A. Greiner, and S. Melchionna, Lattice Boltzmann modeling of water-like fluids, *Front. Phys./Comp. Phys.* **2**, 22 (2014) [DOI: 10.3389/fphy.2014.00022].
4. H. Gould and J. Tobochnik, *An Introduction to Computer Simulation Methods. Applications to Physical Systems* (Addison-Wesley, Boston, 1988).
5. L.O. Landau and E.M. Lishitz, *Statistical Physics* (Pergamon, Oxford, 1980).
6. S.Y. Liem, P.L.A. Popelier, and M. Leslie, Simulation of liquid water using a high-rank quantum topological electrostatic potential, *Intern. J. of Quant. Chem.* **99**, 685 (2004) [DOI: 10.1002/qua.20025].
7. K. Kiyohara, K.E. Gubbins, and A.Z. Panagiotopoulos, Phase coexistence properties of polarizable water models, *Mol. Phys.* **94**, 803 (1998) [DOI: 10.1080/002689798167638].
8. Y. Wu, H.L. Tepper, and G.A. Voth, Flexible simple point-charge water model with improved liquid-state properties, *J. Chem. Phys.* **124**, 024503 (2006) [DOI: 10.1063/1.2136877].
9. H.J.C. Berendsen, J.R. Grigera, and T.P. Straatsma, The missing term in effective pair potentials, *J. Chem. Phys.* **91**, 6269 (1987) [DOI: 10.1021/j100308a038].

Received 26.12.15

В.С. Савенко, Г.М. Вербицька, Л.А. Булавін

КОМП'ЮТЕРНЕ МОДЕЛЮВАННЯ ПРОЦЕСУ ВИПАРОВУВАННЯ ВОДНОГО РОЗЧИНУ NaCl

Р е з ю м е

Випаровування крапель аерозолів є важливим аспектом науки та промисловості. Хоча теоретичні основи цього процесу були розроблені понад 100 років тому і в наш час доповнені різними поправками, її формули не є повністю релевантними для процесу випаровування: часто вони дають тільки грубі оцінки для складних систем. Комп'ютерне моделювання є придатним інструментом для розрахунку параметрів процесу випаровування аерозолів. У цій статті ми представили модель для комп'ютерного моделювання процесу випаровування іонного розчину. Сіль NaCl було вибрано на роль електроліту через свою простоту і широке застосування. Процес моделювання ґрунтується на методі Монте-Карло. Ми розглядаємо температуру T, тиск навколишнього середовища та концентрацію NaCl як вхідні параметри моделювання та коефіцієнт випаровування як вихідний. Для моделювання взаємодії між молекулами води були використані потенціали Стокмайера і Леннард-Джонса. Щоб оцінити ефективність запропонованої моделі, коефіцієнт випаровування було визначено експериментально. Було показано, що отримані експериментально коефіцієнти випаровування мають той самий порядок величини, що й розраховані за допомогою комп'ютерного моделювання.